

An Automatic Shape Optimisation Method for Loaded Contacts Applied to Spline Couplings

Dr John M W Baynham, BEASY Ltd ¹

Mr Christian Duchow, formerly of Wessex Institute of Technology

Dr Colin McFarlane, Ton 7 Technologies Ltd ²

1 j.baynham@beasy.com

2 tonseven@aol.com

Synopsis

Contact geometry has a strong influence on the load capacity and life of transmission elements, such as spline couplings, that rely on power transfer via contacting conformal surfaces.

This paper describes a new numerical tool that automatically generates the necessary contact geometry for the required distribution of contact stress and load transfer.

As an example, the method is applied to a spline coupling for which experimental measurements are available.

Introduction

This paper is based on the results of a short industrial research project performed at the Wessex Institute of Technology. The project focused on the automatic optimisation of the contact geometry of torque transmitting spline couplings. The commercial software BEASY, which applies the boundary element method (BEM), and which was previously enhanced for the analysis of spline couplings as part of a DTI sponsored research programme, Reference 1, was used as a black box solver during the project.

Spline couplings are very dependent on the nature of the contact between the teeth and the resulting contact stress distribution. For teeth that are conformal in the unloaded condition, the deflections due to loading are often sufficient to produce a mal-distribution of contact stress with very high localised peak values that can severely limit the capacity and life of the coupling due to fatigue or wear. For high performance heavily loaded couplings therefore, modifications such as lead corrections and profile relief are often used to improve the contact stress distribution and so improve the performance of the coupling. The problem with any new design is knowing how to modify the shape of the contacting surfaces to obtain the optimum performance. This paper describes initial results from a method that automates the process and which will enable the designer to tailor the optimisation criteria to the requirements of the particular design. Since the method uses the BEM solver, in addition to producing details of the required corrections, the full stress state and a wear rate assessment of the coupling are also obtained.

Basis of the Approach

Completely different algorithms are used in BEM simulation of conforming and non-conforming contact (References 1 and 2). For conforming spline couplings the contacting surfaces of the two parts are represented using a double layer of identical elements. These pairs of elements have nodes at identical positions in the unloaded state (which is why the approach is also known as *node-to-node contact*). However, the method allows definition of an *initial gap* between pairs of nodes. The initial gap is a boundary condition applied to every element within the area of contact. The use of a non-zero positive initial gap allows representation of surfaces that are separated by some relatively small distance in the unloaded state. The initial gap may vary over the contact area and a negative initial gap implies interference. Since very small changes of shape have a significant effect on contact stresses, it has been found that the BEM initial gap boundary condition provides a quick and effective way of applying contact geometry modifications and analysing their effect on coupling stresses.

The validity of this approach was confirmed at Reference 3 where BEM analyses using initial gaps to simulate lead corrections were compared with test results for a torque loaded strain gauged lead corrected test spline coupling, e.g. see Figure 1 and 2 from Reference 3 that show comparisons for root torsional and tooth bending stress.

With an effective way of assessing the effect of contact geometry modifications, the next logical step was to develop a means of specifying them and the method developed is now described in the next section.

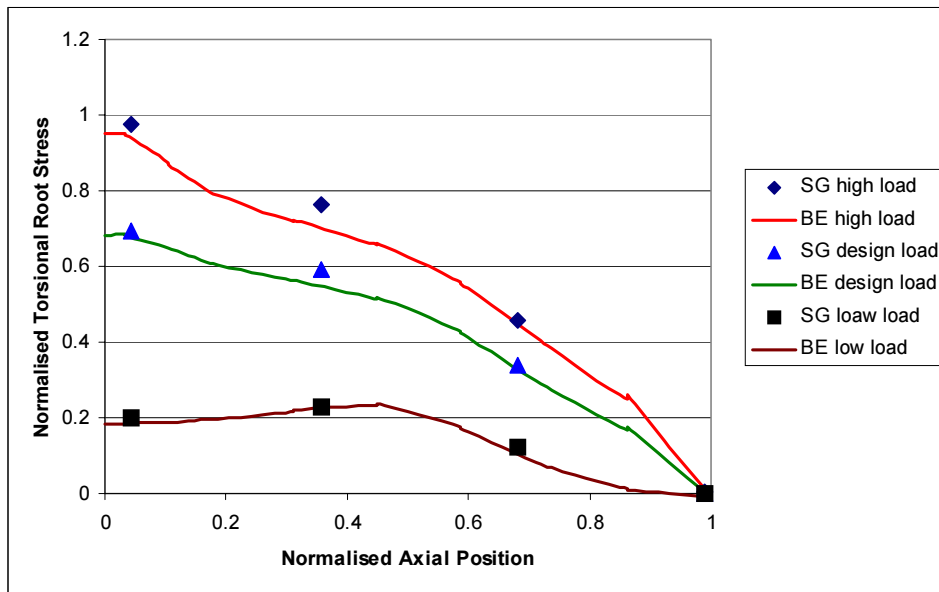


Figure 1 Axial distribution of root torsional stress for three load cases from Reference 3

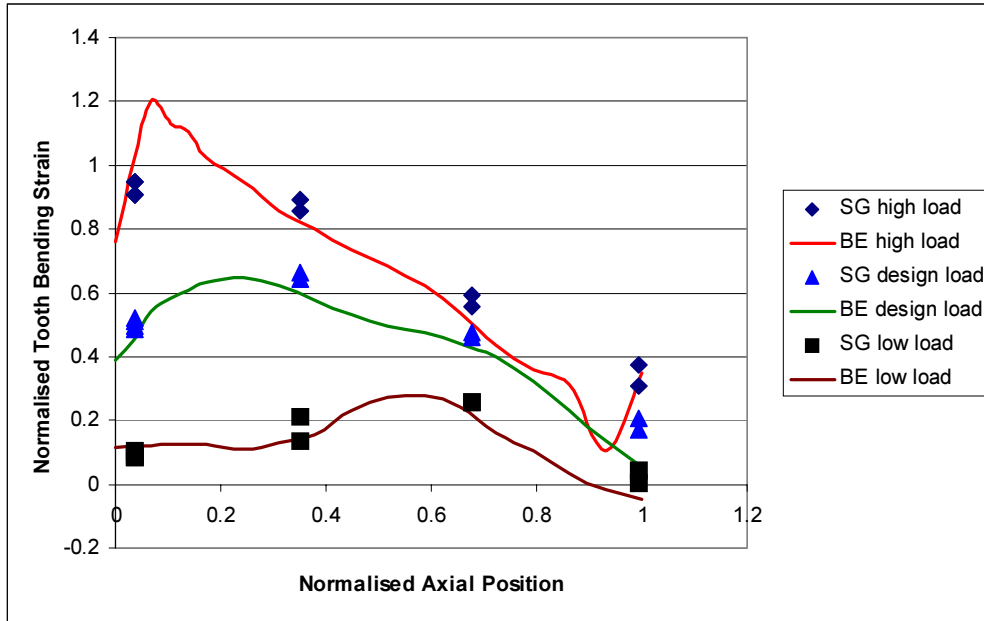


Figure 2 Axial distribution of tooth bending stress for three load cases from Reference 3

The Contact Optimisation Wizard

The starting point is a complete BEM mesh of the coupling, with restraints and loads, and with identification of the contacting surfaces. The initial gap defined on the contacting surfaces may be zero everywhere, but need not be zero.

The “contact optimisation wizard” takes the data file containing the BEM mesh, asks the user for some controlling data, and then starts the process of automatically adjusting the shape. This process involves the steps:

- Perform simulation of the current shape
- Inspect the stress distribution
- Adjust the initial gap boundary conditions
- Write a new data file containing the adjusted shape
- Perform simulation of the new shape
- ...and so on

There are controls that terminate the process when convergence is achieved. All the intermediary files are retained, so progress of the iterative process can be reviewed.

The end result of the successful process is a data file containing values of initial gap that produce something approaching the target stress distribution. The target stress distribution used in this study is constant contact pressure since this equalises loading along the length of the teeth.

Other Features of the Wizard

The wizard visually displays results such as contact stress, initial gap, slip, and other quantities of interest. Since the aim is to provide a practical tool, the final set of initial gap values can be displayed in the form of a lead correction diagram, with the data also going to a text file.

The wizard calculates wear using:

$$h = k \int p \cdot ds$$

where:

h = thickness removed

k = a wear coefficient

p = pressure

s = slip

After an optimised design has been selected, the wizard allows investigation of the effects of accumulated wear. This process involves the steps:

- Perform simulation of the initial shape
- Use contact pressure and slip to calculate wear per cycle
- Accumulate wear for a given number of cycles
- Adjust the initial gap boundary conditions to include accumulated wear
- Write a new data file containing the worn shape
- Perform simulation of the new shape
- ...and so on

Starting from an existing design, the wizard can also be used to assess the effects of manufacturing tolerances as defined by the user. This process involves the following steps:

- Perform simulation of the initial shape
- Adjust the initial gap boundary conditions to include manufacturing tolerances
- Write a new data file containing the as-manufactured shape
- Perform simulation of the as-manufactured shape

Shape Optimisation Methodology

Although in principle it may be possible to use optimising software to control the way the shape is changed, in this work a simple approach was taken as follows.

If “high” stress is observed at a position, the initial gap is increased.

If “low” stress is observed at a position, the initial gap is reduced.

This *unconstrained* approach results in a completely free distribution of metal-off values. Since such a distribution may not be easy or economic to manufacture or provide the required stress

distribution, an alternative *constrained* method was developed in which the entire tooth height is assigned the same initial gap.

Deciding how much to change the initial gap is crucial, since a bad choice can make the iterative process unstable. In this work the change of the gap at some selected position depends on the current gap, the stress value, and also the *overall* stress distribution. (The overall stress distribution is used to judge whether a stress value is *high* or *low*). Various algorithms were tested, some of which allow only increase of the gap, some of which also decrease it. For practical reasons it was decided to allow only *positive* initial gap values, since this corresponds to *removal* of metal.

An Example

The example selected is a helical coupling with 18 teeth for which experimental data is available, Reference 3. Making the assumption that there is cyclic symmetry allows a single tooth to be meshed, see Figure 3.

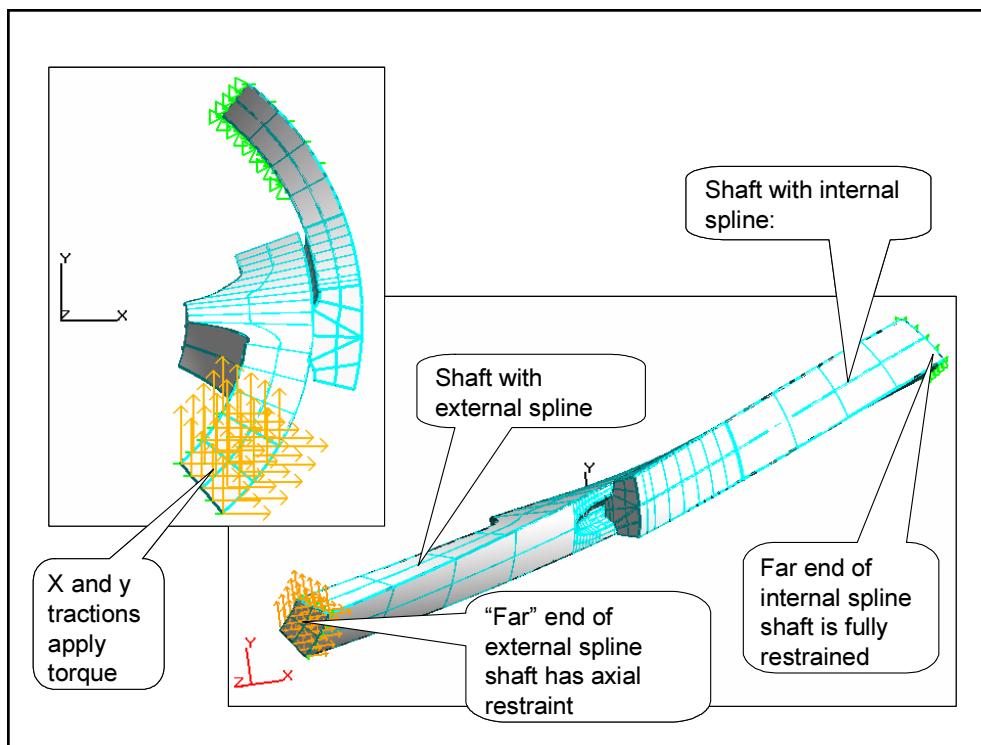


Figure 3 Cyclic Symmetry Model of Spline Coupling showing Boundary Conditions

As shown at Figure 3, the end of the internal spline shaft is completely restrained, and a torque is applied to the end of the external spline shaft, which is also restrained against axial movement. The material of both components is steel. A static friction coefficient of 0.5 was used, with dynamic friction coefficient set to 0.25.

Analyses using both the *unconstrained* and *constrained* optimisations have been carried out and compared with results for the model with uncorrected geometry (zero initial gaps) and the model with lead corrections equal to the test spline.

As described in the previous section, the *unconstrained* optimisation places no restrictions on the geometry modifications while the *constrained* optimisation restricts the modifications to having a constant gap for the full height of the tooth, but places no restrictions in the axial direction.

The corrections used on the lead corrected test spline have been shown, Reference 3, to produce equal loading along the length of the teeth at the design load and can therefore be used as a standard to judge the effectiveness of the optimisation process.

The same mesh and load-stepping algorithms were used in all solutions.

Results

Figure 4¹ shows the contact pressure distribution for the solution with no corrections (*zero initial gap*) and no optimisation. This is equivalent to a coupling with conformal contact along the full length of the teeth in the *unloaded condition*.

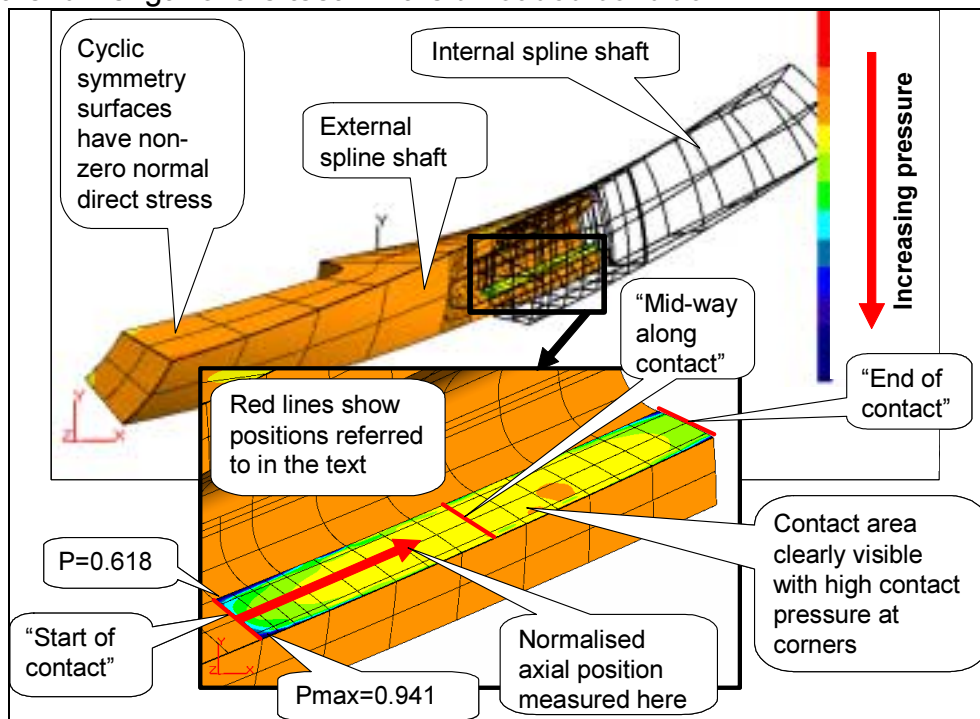


Figure 4 Distribution of Normalised contact stress for zero initial gaps and no optimisation

This shows high peak stresses at both ends of the contact with the highest stresses occurring at the corners at the start of contact; the extent of this mal-distribution of contact

¹ Note that torque flows from the external spline to the internal spline i.e. left to right along the contact zone in the figures.

stress can be fully appreciated by considering the axial distribution of contact stress at the tooth mid-height as shown at Figure 5A, and the distribution of contact stress along the tooth height at the start of contact, at the mid-way of contact and at the end of contact as shown at Figure 5B

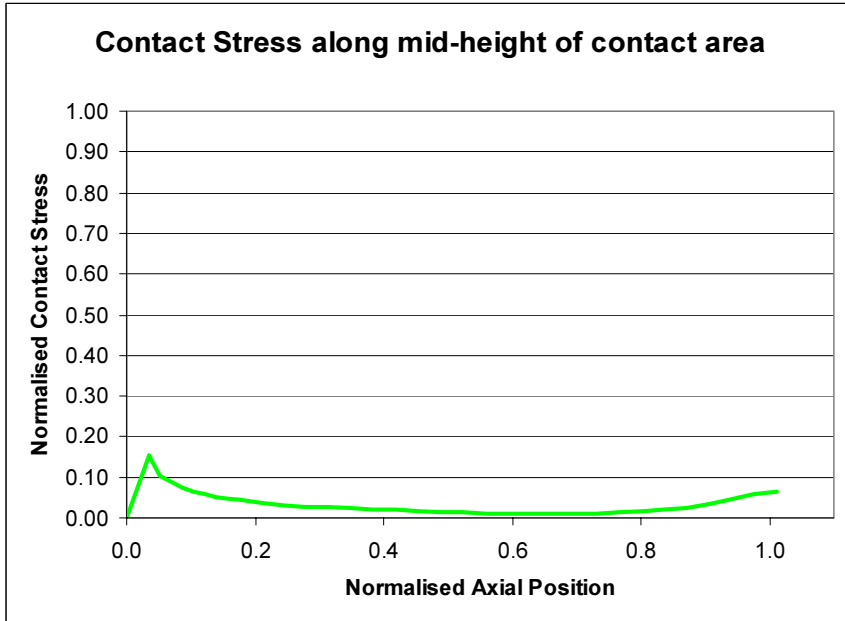


Figure 5A Axial Distribution of Contact Stress (zero initial gap)

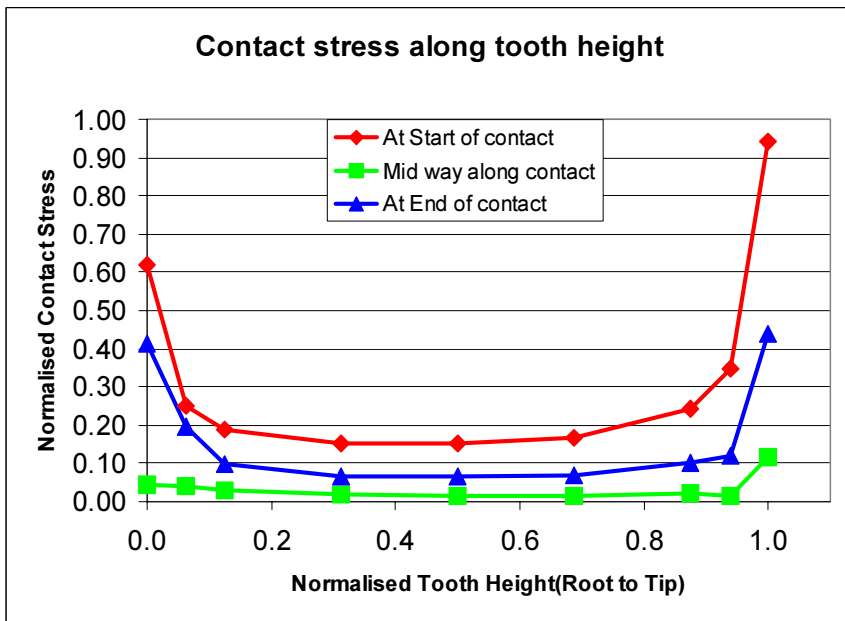


Figure 5B Distribution of Contact Stress along the Tooth Height (zero initial gap)

These show very high peak stresses at the tip and inner positions at the start of contact, low contact stress along the mid-height of the tooth and increased stresses at the inner and tip

positions at the end of contact. This indicates that the torque transfer is mainly occurring at the start and end of contact with the middle of the contact length making little contribution.

Next, considering the results for the lead corrected test spline to show the improvement that corrections can make to the contact stress distribution. Figure 6 shows that the corrections have removed the high end – of – contact peaks and produced a much smoother stress distribution and Figure 7, by comparing the tooth mid-height axial stress distributions of the uncorrected and corrected analyses, shows that the corrections produce a much more constant pressure distribution along the length of the spline. It has been shown experimentally, Reference 3, that the lead corrections used produce a linear transfer of torque from the external spline to internal spline at the design load, inferring a fairly constant axial contact stress distribution and this is predicted by the current analysis.

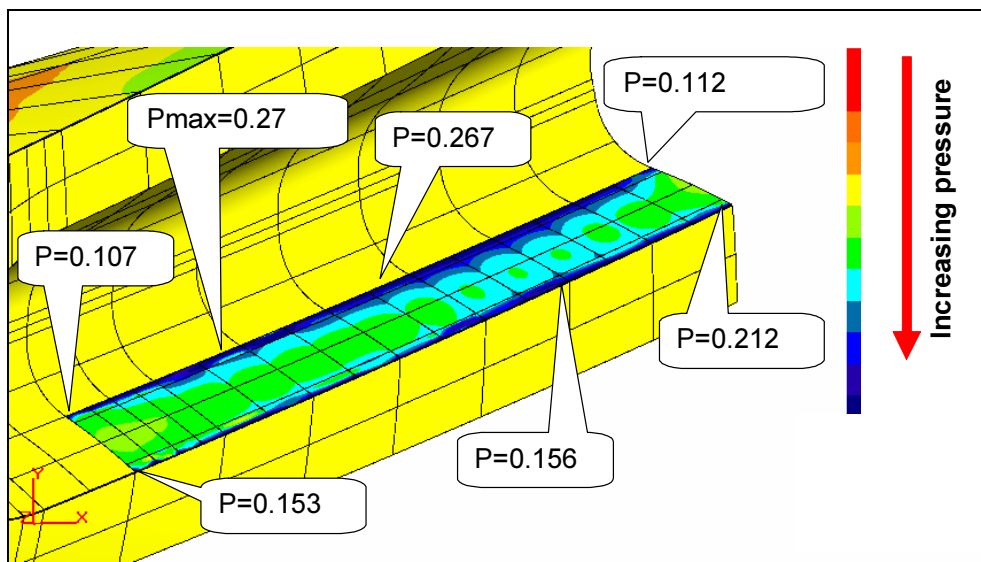


Figure 6 Distribution of normalised contact stress for lead corrected spline with no optimisation

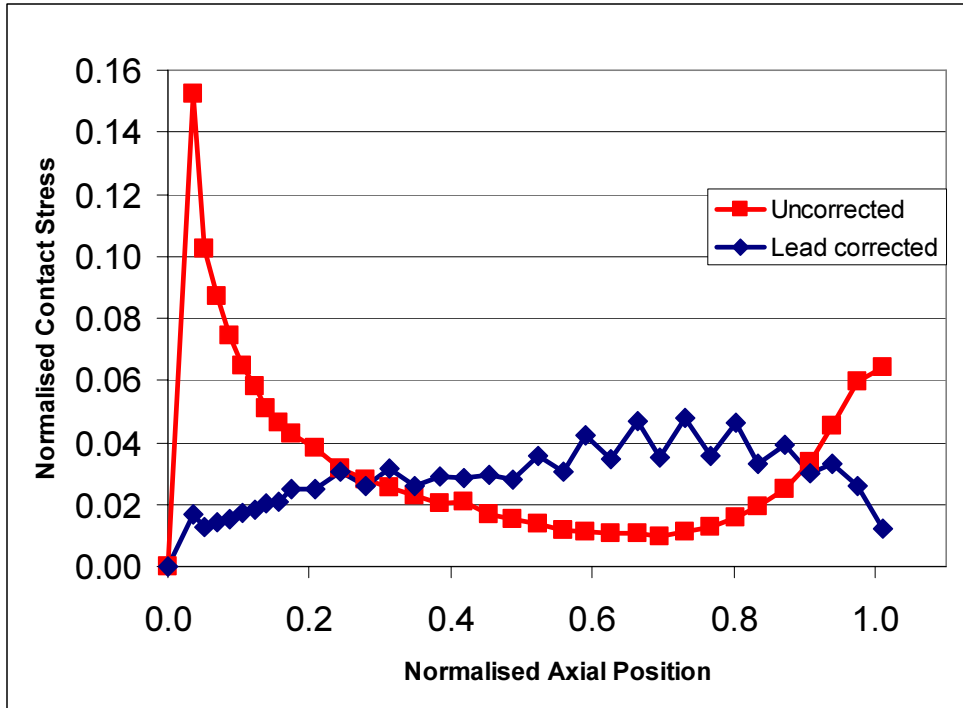


Figure 7 Comparison of the uncorrected (zero initial gap) and lead corrected tooth mid-height axial distributions of contact stress

As described earlier, two optimisation methods were assessed, the *unconstrained* and *constrained* approaches and the resulting contact stress distributions are shown at Figures 8 and 9 respectively.

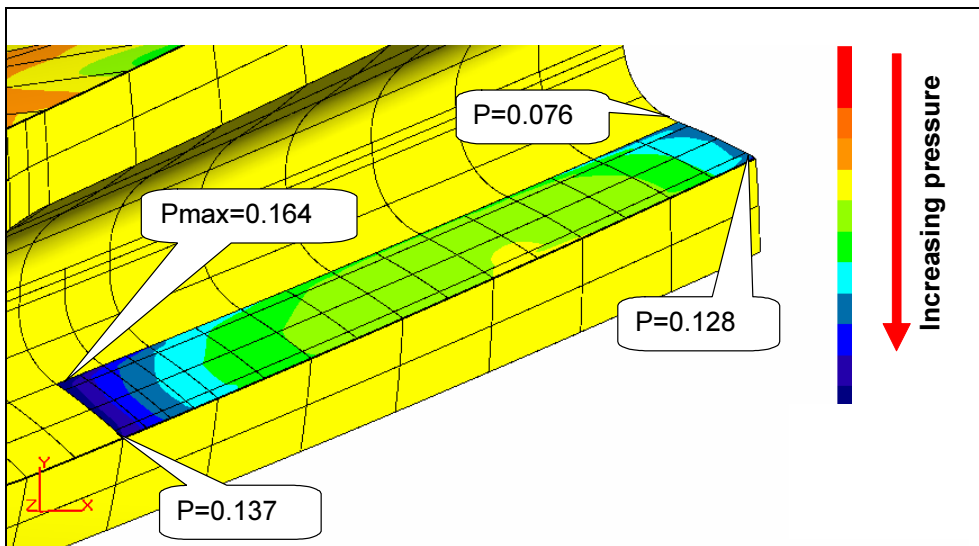


Figure 8 Distribution of normalised contact stress for unconstrained optimisation, after 29 iterations

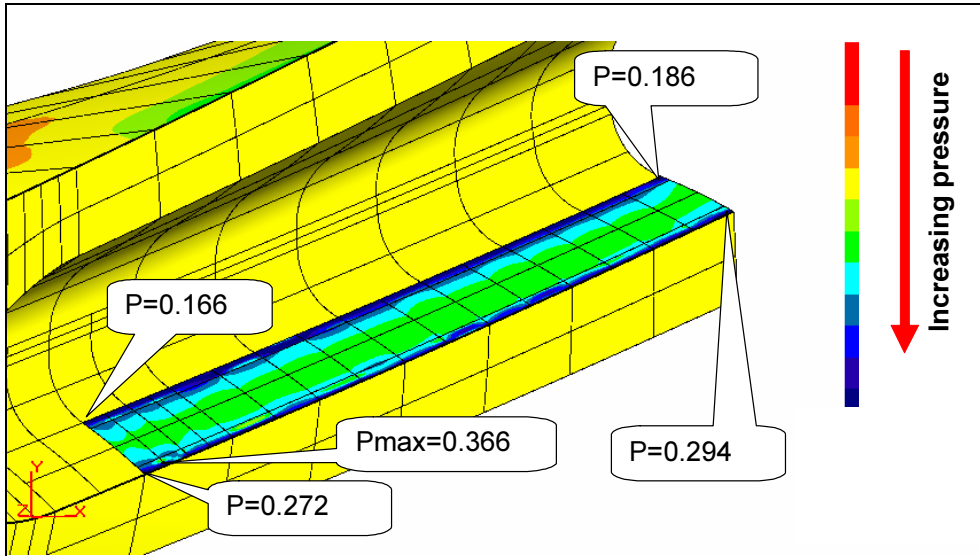


Figure 9 Distribution of normalised contact stress for constrained optimisation, after 59 iterations

Inspection of the figures show that both optimisations make significant improvements to the contact stress distributions relative to the uncorrected (zero initial gap) analysis shown at Figure 4. This can also be seen at Figures 10 and 11 that show the axial tooth mid-height and start of contact tooth root to tip contact stress distributions. The unconstrained method converges to a distribution almost constant from tooth root to tip, but with significant peak stresses – similar in magnitude to the mid-height zero initial gap values - at the start and end of contact. Both the constrained and lead corrected solutions produce almost constant axial contact stress distributions, but with peak stresses at the tooth root and tip, the constrained peak values being greater than the lead corrected values. Comparison of Figures 6 and 9 also shows that the peak stress value of the lead corrected spline occurs at the root some distance from the start of contact whilst the peak value for the constrained optimisation occurs at the tip close to the start of contact.

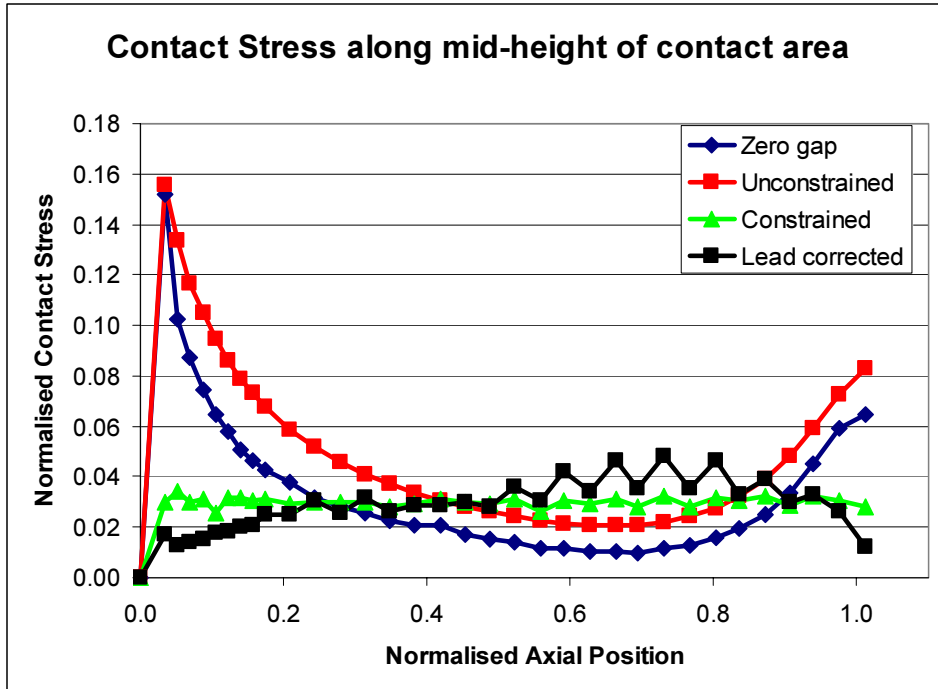


Figure 10 Comparison of mid-tooth-height axial distribution of contact stress

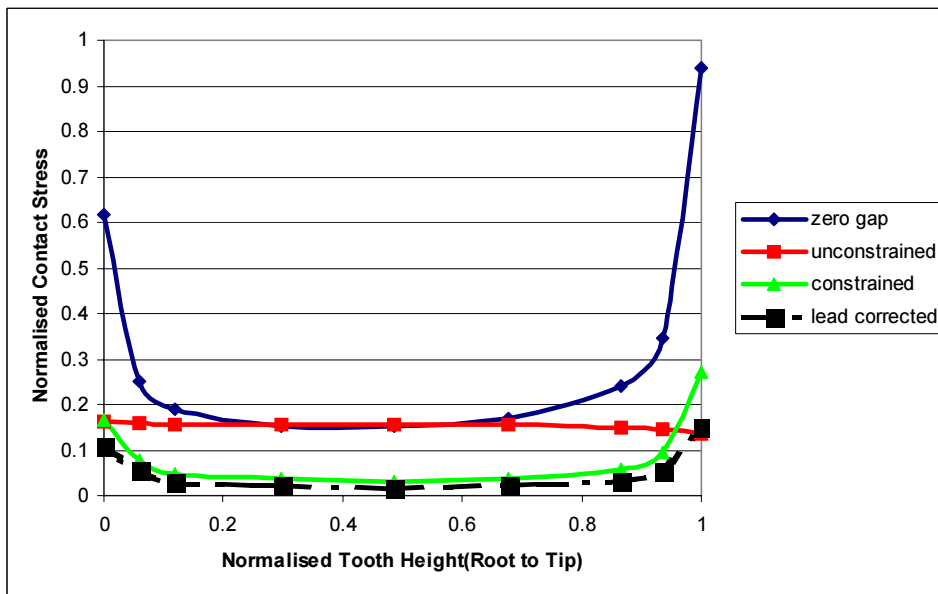


Figure 11 Comparison of tooth root to tip contact stress distributions at the start of contact

The effect of the contact stress distributions on the torque transfer from the external to the internal spline is shown at Figure 12. For the lead corrected spline, as would be expected

for an almost constant axial distribution of contact stress, there is an almost linear transfer - indicating equal loading along the length of the teeth - and good agreement with the strain gauge measurements from Reference 3. The constrained optimisation shows a similar distribution whilst the unconstrained and zero initial gap results show a high initial rate of torque transfer with around 50% of the torque being transferred within the first 25% of the contact length, indicating heavily loaded teeth at the start of contact and under utilisation of the remaining tooth length. The poorer performance of the unconstrained optimisation is due to the non-constant axial distribution of contact stress with peak values at the start of contact. This results in a torque distribution similar to the uncorrected (zero initial gap) results. Similarly, the difference between the constrained optimisation and the lead corrected spline is due to a slightly higher initial rate of torque transfer for the constrained optimisation due to a slightly greater contact stress at the start of contact.

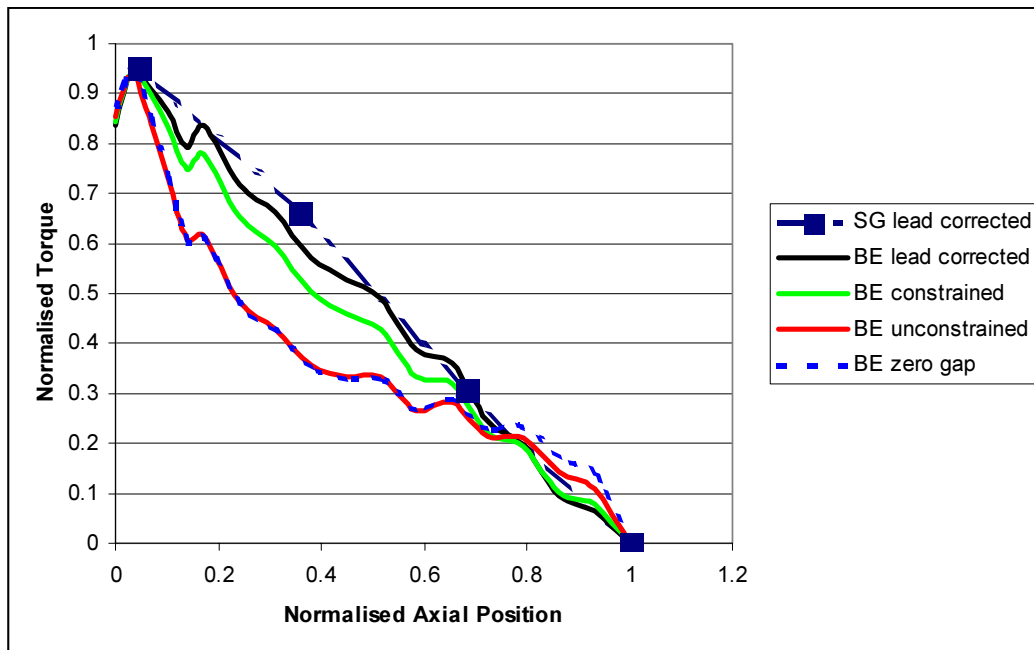


Figure 12 Comparison of torque axial distributions

The initial gap distribution obtained from the constrained analysis is compared with the lead corrected gap distribution at Figure 13.

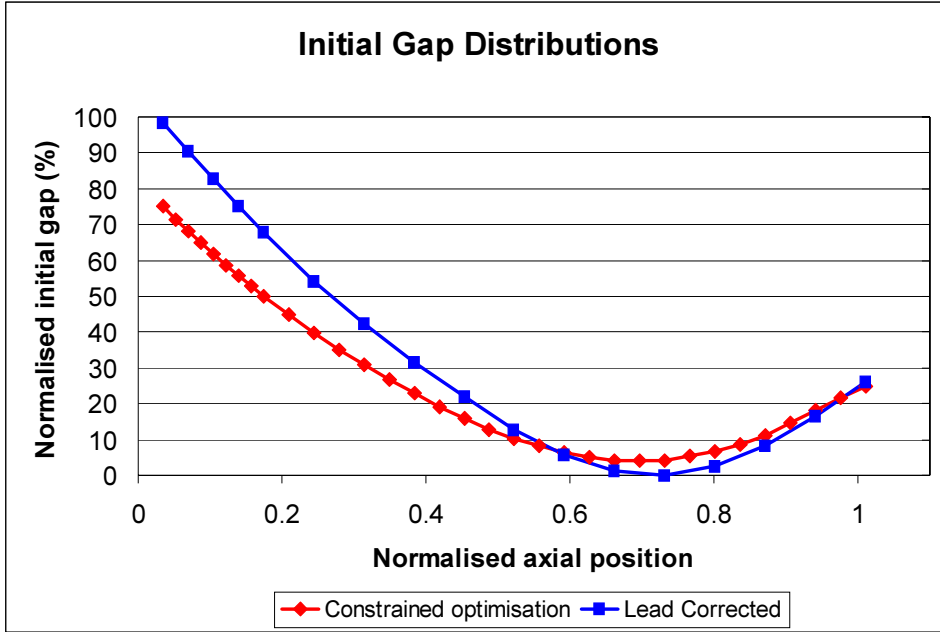


Figure 13 Comparison of constrained optimisation and lead corrected initial gaps

The distributions of relative slip between the contacting surfaces at the end of loading are compared at Figures 14 and 15 and show that similar values of maximum slip values are predicted for all four cases with the unconstrained optimisation producing the lowest value.

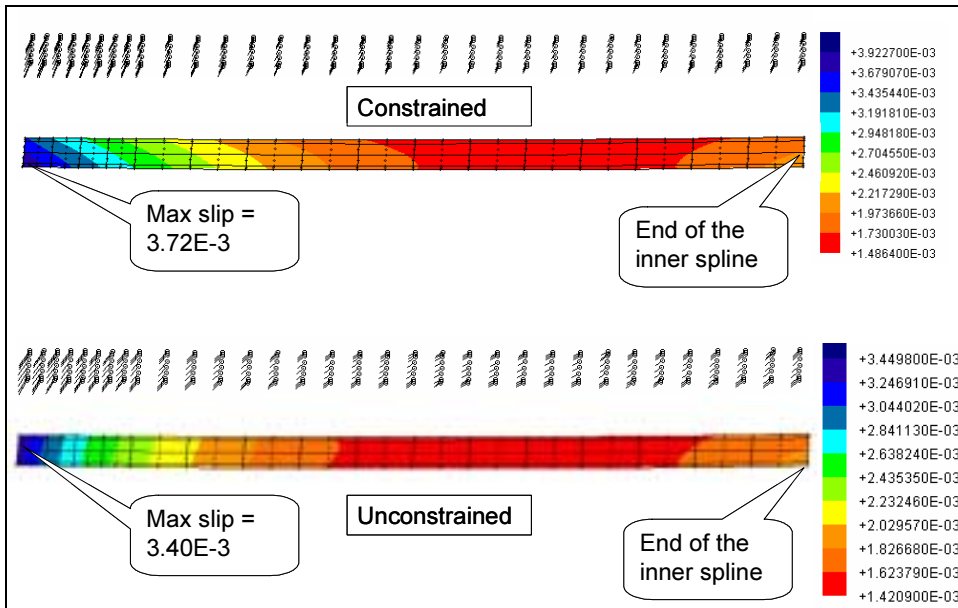


Figure 14 Comparison of slip for constrained and unconstrained optimisations

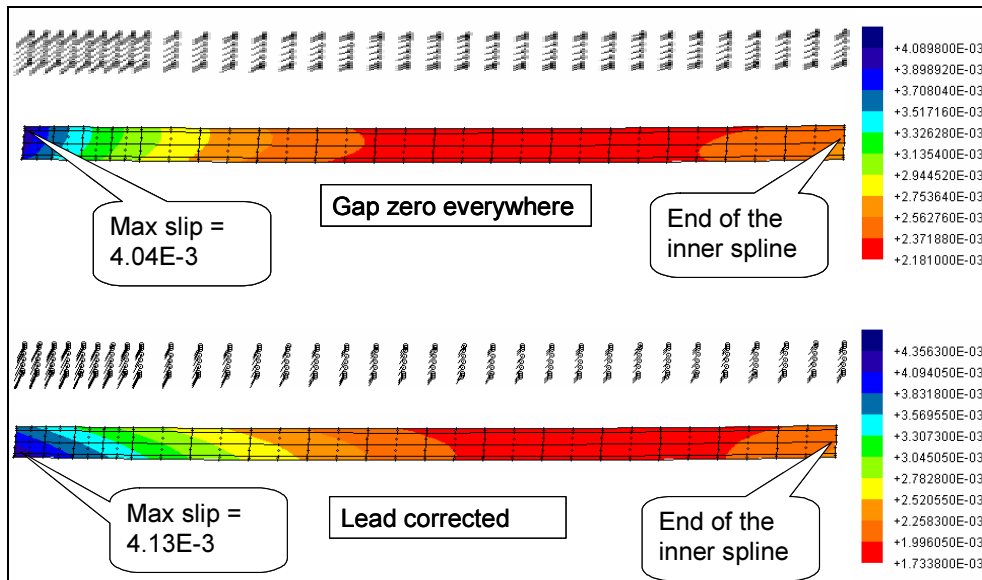


Figure 15 Comparison of slip for zero initial gap and the lead corrected couplings

The distributions of wear per cycle are shown at Figures 16 to 19. The wear analyses are based on an arbitrary wear coefficient of 10^{-7} , so should only be used for comparative purposes. The highest wear per cycle, 16×10^{-5} , is predicted for the spline with no lead correction (zero initial gap), Figure 16. The constrained optimisation reduces this by more than 60%, to 6×10^{-5} , Figure 17, while the lead corrected spline is still better, reducing the maximum wear to 4.9×10^{-5} per cycle, Figure 18. However, the unconstrained optimisation produces the greatest improvement over the uncorrected spline, reducing the wear by 86%, to 2.25×10^{-5} per cycle Figure 19.

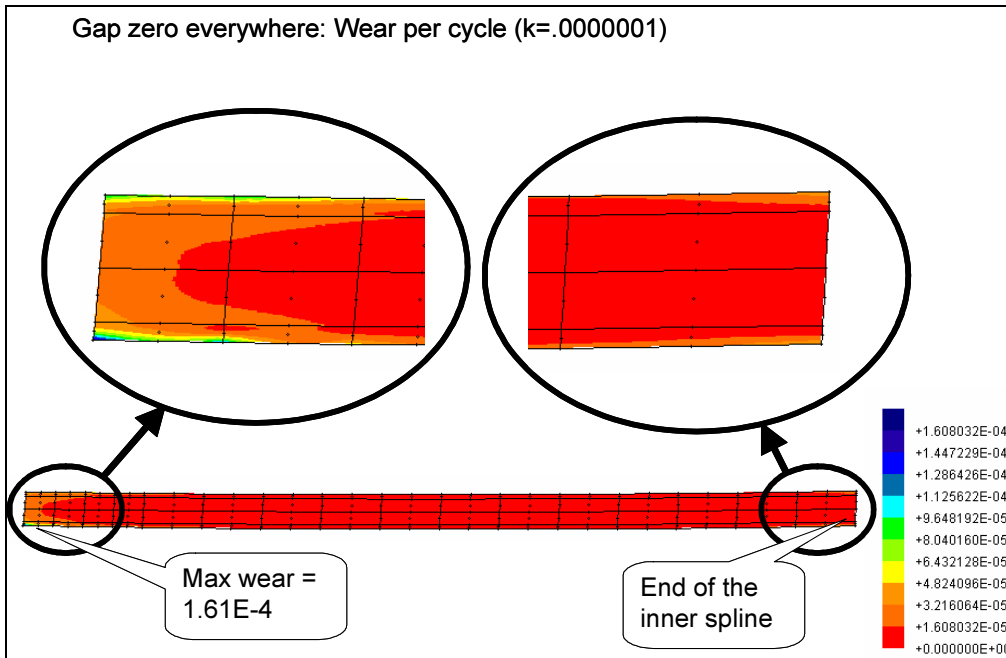


Figure 16 Predicted wear per cycle for uncorrected (zero initial gap) spline

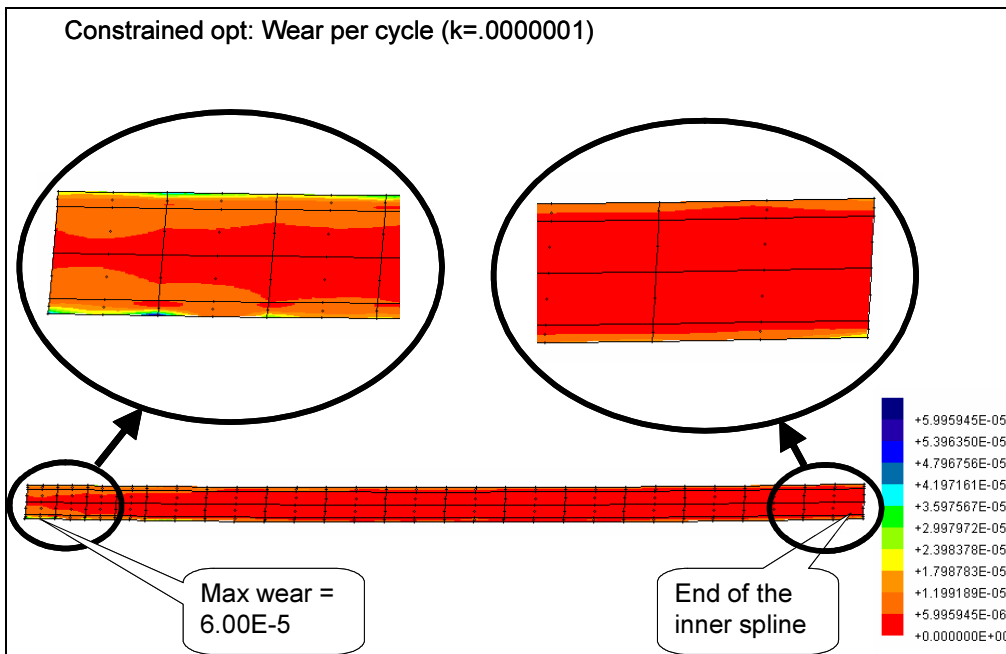


Figure 17 Predicted wear per cycle for constrained optimisation

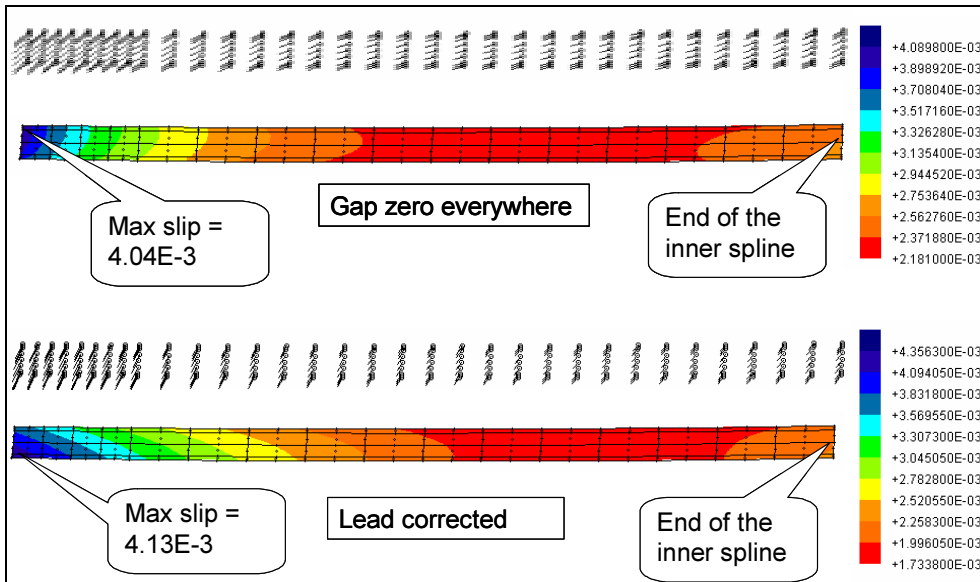


Figure 18 Predicted wear per cycle for lead corrected spline

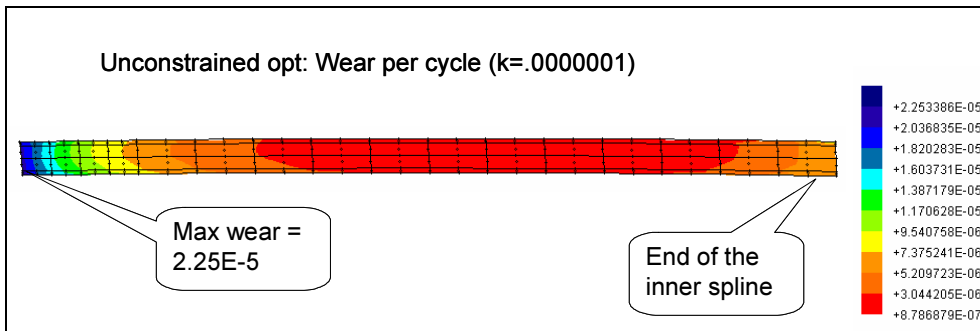


Figure 19 Predicted wear per cycle for unconstrained optimisation

Discussion and Conclusions

The results show that the optimisation technique can significantly improve both the contact stress distribution and the predicted wear performance of spline couplings.

The constrained optimisation converges to a solution that provides an almost constant rate of torque transfer and therefore constant loading along the full tooth length. This solution is also very comparable to the lead corrected test spline that has been shown experimentally to have equal axial tooth loading. The constraint of constant gaps at each axial position and the resulting axial gap distribution, which is similar to that used on the lead corrected spline, is also considered to be practical for manufacture.

The unconstrained optimisation, interestingly, does not improve the axial distribution of tooth loading from that of the uncorrected (zero initial gap) solution because it converges

to a solution that retains a peak contact stress at the start of contact. The reason for this may be related to the way in which convergence is presently assessed, and it may be possible to improve on this result.

This unconstrained solution produces an almost constant pressure distribution from tooth root to tip, while the constrained solution, due to the use of constant gaps from tooth root to tip at each axial position, produces peak stresses at the roots and tips. The magnitudes of the peaks are small compared to the uncorrected solution and in practical terms probably of secondary importance to the achievement of constant loading along the length of the teeth. If required, however, with some development of the method they could be eliminated.

In terms of predicted wear, the unconstrained optimisation produces the greatest improvement relative to the uncorrected coupling, however, the constrained and lead corrected solutions also produce significant improvements.

The results indicate that for improving torque capacity, the constrained optimisation would produce the best results, while, if wear was the major design factor, the unconstrained optimisation may be preferable. It is envisaged that the method could be developed to have optimisations suited to different performance requirements and manufacturing capabilities and which could be selected at the discretion of the designer.

Overall, it is concluded that the optimisation technique provides the basis for an effective design tool that has the potential to automate the design of spline tooth geometry modifications thereby ensuring design consistency and reliability.

References

1. **Development of Analysis Technology for Spline Couplings**, R.A. Adey , J. Baynham and J.W. Taylor, Coupling and Shaft Technology for Aerospace Transmissions Seminar, IMechE, 9th June 1999
2. **Modeling Contact Surface Edge Effects Using Boundary Elements**, Thomas J. Curtin , John M. W. Baynham and Robert A Adey. Proceedings of the ASME High Cycle Fatigue Conference 2003.
3. **The Comparison of the Boundary Element Analysis of a High Performance Spline Coupling with Experimental Measurements**, C. McFarlane, E.J. Williams & T. Hyde, Coupling and Shaft Technology for Aerospace Transmissions Seminar, IMechE, 9th June 1999